

PI3K δ as a novel therapeutic target in pathological angiogenesis

Wenyi Wu^{1,2}, Guohong Zhou^{1,3}, Haote Han¹, Xionggao Huang^{1,4}, Heng Jiang^{1,5}, Shizuo Mukai⁶, Andrius Kazlauskas⁷, Jing Cui⁸, Joanne Aiko Matsubara⁸, Bart Vanhaesebroeck⁹, Xiaobo Xia², Jiantao Wang¹⁰, and Hetian Lei^{10, 1*}

¹Schepens Eye Research Institute of Massachusetts Eye and Ear; Department of Ophthalmology, Harvard Medical School, Boston, MA. USA

²Department of Ophthalmology, Xiangya Hospital, Central South University, Changsha, China

³Shanxi Eye Hospital, Taiyuan, China

⁴Department of Ophthalmology, the First Affiliated Hospital of Hainan Medical University, Haikou, China

⁵Department of Ophthalmology, Second Xiangya Hospital, Central South University, Changsha, China

⁶Massachusetts Eye and Ear, Department of Ophthalmology, Harvard Medical School

⁷Department of Ophthalmology & Visual Sciences, Department of Physiology and Biophysics, University of Illinois at Chicago, Chicago, IL. USA

⁸The University of British Columbia, Canada

⁹Cancer Institute, University College London, London, UK

¹⁰Shenzhen Eye Hospital, Shenzhen Eye Institute, Shenzhen, China

Running title: *PI3K δ in pathological angiogenesis*

*To whom correspondence should be addressed: Hetian Lei, Ph.D., Schepens Eye Research Institute, Harvard Medical School, 20 Staniford Street, Boston, MA 02114. Telephone: 00-1-6179122521, Fax: 00-1-6179120101, email: hetian_lei@meei.harvard.edu.

Abstract

Diabetic retinopathy is the most common microvascular complication of diabetes, characterized by the formation of fibrovascular membranes that consist of a variety of cells including vascular endothelial cells (ECs). New therapeutic approaches for this diabetic complication are urgently needed. Here, we report that in cultured human retinal microvascular (HRECs) high glucose induced expression of p110 δ , which was also expressed in ECs of fibrovascular membranes from diabetic patients. This catalytic subunit of a receptor regulated PI3K isoform δ is known to be highly-enriched in leukocytes. Using genetic and pharmacological approaches, we show that p110 δ activity in cultured ECs controls Akt activation, cell proliferation, migration, and tube formation induced by vascular endothelial growth factor, basic fibroblast growth factor, and epidermal growth factor. Using a mouse model of oxygen-induced retinopathy, p110 δ inactivation was found to attenuate pathological retinal angiogenesis. p110 δ inhibitors have been approved for use in human B-cell malignancies. Our data suggest that antagonizing p110 δ constitutes a previously-unappreciated therapeutic opportunity for diabetic retinopathy.

Introduction

Diabetic retinopathy is the most common of microvascular complication of diabetes and a leading cause of blindness (1). Pathologic angiogenesis is associated with proliferative diabetic retinopathy (PDR), an advanced stage of diabetic retinopathy (2). Pro-angiogenic molecules including basic fibroblast growth factor (bFGF) (3), epidermal growth factor (EGF) (4), and vascular endothelial growth factor (VEGF) (5) promote proliferation and migration of vascular endothelial cells (ECs), initiating pathologic angiogenesis. Currently available treatments of diabetic retinopathy include neutralizing VEGF in the vitreous either using antibodies against VEGF (ranibizumab, bevacizumab) or a recombinant fusion protein consisting of an antibody Fc fragment fused to the extracellular domains of VEGF receptor (VEGFR) 1 and -2 (aflibercept) (6-8). These anti-VEGF agents reduce neo-vascular growth and lessen vascular leakage; however, resistance to these drugs or recurrence of disease is observed in a significant number of patients with PDR (1,9), and

new therapeutic approaches are urgently needed.

During the process of angiogenesis, a series of pro-angiogenic intracellular signaling cascades are rapidly activated including the phosphoinositide 3-kinase (PI3K)/Akt pathway (10,11). PI3Ks have been divided into three classes (I, II and III) based on their structural features and lipid substrate preference (10). Class IA PI3Ks are composed of a p110 catalytic subunit (p110 α , p110 β or p110 δ) bound to one of five p85 regulatory subunits (12). Whereas p110 α and p110 β are ubiquitously expressed, p110 δ is mainly expressed in white blood cells (13) and controls immune functions (14-16). p110 α has been reported to be the main regulator of angiogenesis (17) with a modest role of p110 β (18). A role for p110 δ in angiogenesis has not been reported. Small molecule inhibitors of p110 δ are being explored clinically as pharmacologic treatments for inflammatory disease and cancer (19), and three compounds that share the ability to target p110 δ have recently been approved for use in human B-cell malignancies (12,20).

However, while expression of p110 δ is known to be expressed at low levels in other cells than leukocytes including fibroblast-like cells (21) and ECs (22), and become further induced by tumor necrosis factor (TNF) α in ECs (22), its role in these tissue contexts is unknown. In the current study we uncover functional roles of p110 δ activity in cultured ECs and in pathological angiogenesis in a mouse model of oxygen-induced retinopathy (OIR).

Methods

Major reagents

VEGF-A (further referred to as VEGF) (Catalog number (Cat): 293-VE-010), bFGF (Cat : 233-FB), EGF(Cat: 236-EG) and PDGF-A (Cat: 221-AA) were purchased from R&D systems (Minneapolis, MN). Antibodies against p110 α (Cat: 4249), p110 β (Cat: 3011), p110 δ (Cat: 34050), Akt (Cat: 9272), phospho-Akt (S473) (Cat: 4058), CD31 (Cat: 3528), and VE-Cadherin (Cat:2500) were purchased from Cell Signaling Technology (Danvers, MA). L-glucose (Cat: G5500) and D-glucose (Cat: G7021) were purchased from Sigma (St. Louis, MO); idelalisib was purchased from APExBIO (Cat: CAL101, Houston, TX). The primary antibody against β -Actin (Cat: sc-47778) and secondary antibodies of

horseradish peroxidase (HRP)-conjugated goat anti-rabbit IgG (Cat: sc-2004) and anti-mouse IgG (Cat: sc-2005) were purchased from Santa Cruz Biotechnology (Santa Cruz, CA). Enhanced chemiluminescence substrate for detection of HRP was obtained from Thermo Fisher Scientific (Cat: 34580, Waltham, MA). Alexa fluorescence-594-conjugated mouse endothelial specific isolectin B4 (IB4) was purchased from Life Technology (Cat: 112413, Grand Island, NY). High-fidelity Herculase II DNA polymerases were from Agilent Technologies (Cat: 600677, Santa Clara, CA).

DNA constructs

The three 20nt target DNA sequences preceding a 5'-NGG protospacer-adjacent motif (PAM) sequence at exon 4 in the human genomic *PIK3CD* locus (NG_023434) (23) were selected for generating single-guide RNA (sgRNA) for SpCas9 targets. The control sgRNA sequence (5'-TGCGAATACGCCACGCGATGGG-3') was designed to target the *lacZ* gene from *Escherichia coli* (24). The lenti-CRISPR v2 vector (25) was purchased from Addgene (23) (Cat. 52961, Cambridge, MA).

To express SpGuides in the targeted cells, the top oligos 5'-CACCG-20nt (target *PI3KCD* DNA sequences PK2 (AGAGCGGCTCATACTGGGCG), PK3 (TGTGGAAGAGCGGCTCATAC), PK4 (TCTTCACGCGGTCGCCCTCA), or the *lacZ* sgRNA sequence)-3' and bottom oligos: 5'-AAAC-20nt (20nt: complimentary target *PI3KCD* DNA sequences or *lacZ* sgRNA sequence)-C-3' were annealed and cloned into the lentiCRISPR v2 vector, respectively. All clones were confirmed by Sanger DNA sequencing using a primer 5'-GGACTATCATATGCTTACCG-3' from a sequence of U6 promoter, which drives expression of sgRNAs.

DNA synthesis and sequencing were performed by Massachusetts General Hospital DNA Core Facility (Cambridge, MA).

Cell culture

Three vials of human primary retinal microvascular endothelial cells (HRECs) isolated from three different donors were purchased from Cell Systems (Cat: ACBRI181, Kirkland, WA) and cultured in Endothelial Growth Medium (EGM)-2 (5 mM D-glucose) (Cat: 213KS-500, Cell Applications, San Diego, CA) or EGM in addition to L-glucose (25 mM)

or D-glucose (25 mM) for a week (26). HRECs were used from passages 6 to 10 for following experiments, and their tissue culture dishes were pre-coated with gelatin-based coating solution (Cat: 6950, Cell Biologics, Chicago, IL). The media were changed every other day. All cells were cultured at 37°C in a humidified 5% CO₂ atmosphere (23,27).

Porcine aortic endothelial cells (PAECs) (26) overexpressing platelet-derived growth factor receptor (PDGFR) α were cultured in DMEM/F12 medium supplemented with 10% fetal bovine serum (FBS, Cat: S11150, Bio-Techne, Minneapolis, MN). Human primary lymphatic endothelial cells (HLECs) were purchased from Cellbiologics (Cat: H6092), and human umbilical vein endothelial cells (HUVECs) were purchased from Cell Applications (Cat: 200-05f). These primary ECs were cultured in EGM-2. Mouse cone photoreceptor cells (661W) were obtained by material transfer agreement from University of Houston (Houston, Texas), RAW264.7 mouse macrophages were purchased from American Type Culture Collection (Cat: TIB-71, Manassas, VA) (28), rabbit conjunctival fibroblasts (RCFs) were a gift of Dr. Andrius Kazlauskas (29), and human embryonic kidney (HEK) 293T cells (HEK 293 containing SV40 T-antigen) from The Dana-Farber Cancer Institute/Harvard Medical School (Boston, MA). Cells of 661W, RAW264.7, RCFs and HEK293T were cultured in high-glucose (4.5 g/l) DMEM supplemented with 10% FBS. The medium used to harvest the lentiviral supernatant from 293T cells was high-glucose DMEM supplemented with 20% FBS. All cells were cultured at 37°C in a humidified 5% CO₂ atmosphere(23,27).

Quantitative PCR

HRECs were plated into six-well plates at a density of 1×10^5 cells per well and treated with EGM in addition of L-glucose (25 mM) or D-glucose (25 mM) for one week. Total RNAs were extracted using the RNeasy Plus Mini Kit (Cat: 74104, Qiagen, Germantown, MD). The levels of *PIK3CD* mRNA were normalized to the levels of *hHPRT1* mRNA. Primers of quantitative PCR synthesized by Integrated DNA Technology (Coralville, IA) were (forward: 5'-GAATCAGAGCGTTGTGGTTG-3', reverse: 5'-CAGAATTGGCACATCTTGGC- 3') for *PIK3CD* and (forward: 50-CCTGGCGTCGTGATTAGTGAT-30, reverse: 50-AGACGTTTCAGTCCTGTCCATAA-30) for

a housekeeping gene *hHPRT1* (human hypoxanthine phosphoribosyltransferase 1) (30).

Western blotting analysis

HRECs at 90% confluence in a 24-well plate were deprived of serum and growth factors for continuous incubation for 8 h, and then some of these cells were treated as desired. After washing twice with phosphate-buffered saline (PBS), cells were lysed. The clarified lysates were subjected to western blot analysis using the appropriate antibodies. Experiments were repeated at least 3 times. Signal intensity was determined by densitometry using ImageJ software (<http://imagej.nih.gov/ij/>; provided in the public domain by the National Institutes of Health, Bethesda, MD) (23).

MTT assay

The toxicity of idelalisib on cell viability was assessed using the 3-(4,5-dimethylthiazol-2-yl)-2,5-diphenyl-2H-tetrazolium bromide (MTT, Cat: M2128, Sigma) assay as described previously(31). Briefly, HRECs were seeded into 96-well plates and incubated for 24 h before exposed to a range of concentrations (0, 5, 10, 15, 20, 25, 30, 35, and 40 μ M) of test articles dissolved in DMSO in 5% FBS-supplemented medium for 24-72 h. Each condition was tested with 6 replicates and all assays were performed in triplicate (31).

Cell proliferation assay

HRECs were seeded into 24-well plates at a density of 30,000 cells/well in an endothelial growth medium kit. After attaching the plates, the cells were starved of growth factors for 8 h, and then treated with idelalisib (10 μ M) with or without VEGF, bFGF and EGF (20 ng/ml each). The treatment was repeated daily. After 48 h, the cells were trypsin detached and then counted in a hemocytometer under a light microscope(23).

Wound healing assay

The wound healing assay was performed as previously described (23) with minor modifications. Once HRECs reached confluence in 48-well plates, they were starved for growth factors for 8 h. After the cell monolayer was scraped with a 200- μ l-sterile pipette

tip, the cells were washed twice with PBS to remove detached cells. The cells were treated with idelalisib (10 μ M) with or without supplement with VEGF, bFGF and EGF (20 ng/ml). The wound was photographed at 0 and 18 h post wounding under a microscope (23).

Tube formation assay

This assay was performed as previously described (23) with minor modifications. Briefly, The collagen gel mixture was added to a 96-well plate (70 μ l/well), which was then incubated for about 60 min at 37°C to let the collagen gel polymerize. After polymerization, HRECs (4.5×10^4) were seeded in each well with their cultured medium maintained at a 37°C incubator. This day was considered day 1. On day 2, the medium was removed and 30 μ l of the gel mixture was added to each well. After incubation for about 60 min at 37°C, the collagen gel was polymerized, and the medium (100 μ l) [EBM supplemented with 0.5% horse serum, 0.1% bovine brain extract supplemented with VEGF, bFGF and EGF (20 ng/ml)] with or without idelalisib (10 μ M). On day 3, the gel was photographed using the EVOS FL Auto microscope (23).

Breeding and Genotyping

6 weeks old heterozygous p110 $\delta^{D910A/D910A}$ C57BL/6J (B6) mice were purchased from Charles River Laboratories (Boston, MA) and were used for breeding to generate wild-type (WT), heterozygous (Het) and mutant p110 $\delta^{D910A/D910A}$ (Mut) pups. Genomic DNA was isolated from P12 mice by boiling tail tips in 100 μ l lysis buffer (0.125 M NaOH, 2 mM EDTA) for 25 min, followed by addition of 100 μ l neutralizing buffer (40 mM Tris HCl, pH 8.0). The supernatant after spin was used for PCR using the following primers (forward, P28F: CCTGCACAGAAATGCACTTCC; Reverse, P28R, AACGAAGCTCTCAGAGAAAGCTG). The expected PCR fragments from mutant and WT mice are 500 bp and 332 bp, respectively (32).

A mouse model of oxygen-induced ischemic retinopathy (OIR)

This experiment was performed as described previously (33,34). Briefly, B6 litters on postnatal day (P) 7 were exposed to 75% oxygen until P12 in an oxygen chamber

(Biospherix, Parish, NY). At P12, intravitreal injections were performed under a microsurgical microscope. One μl of idelalisib (final vitreal concentration 10 μM) or its vehicle (0.1% DMSO) based on 5- μl -vitreal volume was injected. After the intravitreal injection, the eyes were treated with a triple antibiotic (Neo/Poly/Bac) ointment and kept in room air (21% oxygen). At P17, the mice were euthanized and retinas were carefully removed for western blot analysis or fixed in 3.7% paraformaldehyde (PFA). Mice under 6 g of total body weight were excluded from the experiments. Retinal whole mounts were stained overnight at 4°C with the murine-specific EC marker IB4-Alexa 594 (red) (33). The images were taken with an EVOS FL Auto microscope.

Enzyme-linked immunosorbent Assay (ELISA)

This experiment was performed by following the instruction of a mouse VEGF quantikine ELISA kit (Cat: MMV00, R & D System). Briefly, clarified vitreous (5 μl) from each eye from P17 mice with or without experiencing OIR was diluted with PBS into 50 μl , which was added into each well. In addition, 50 μl standard was also added to each well, and incubated at room temperature for 2 h. Then, after the wells were washed with wash buffer for 5 times, 100 μl conjugate from the kit was added to each well, and incubated at room temperature for 2 h. After wash for 5 times, 100 μl substrate solution was added to each well and incubated for 30 min. Then, 100 μl of stop solution was added into each well. Finally, the plate was read at 450 nm within 30 min (35).

Examination of idelalisib toxicity in mouse eyes

At P12, five pups were anesthetized and underwent intravitreal injections as described above. A single dose of 1 μl of 50 μM idelalisib stock (dissolved in 0.1% DMSO) was injected. Control injections were performed with 1 μl of the 0.1% DMSO vehicle. Based on the notion that the mouse vitreous volume is 5 μl , this is expected to give rise to an initial final vitreal concentration of 9-10 μM , which is expected to be further diluted over time.

Four weeks later, electroretinography (ERG) (by light/dark adaptation, using a DIAGNOSYS ColorDome containing an interior stimulator), optical coherence

tomography (OCT), and fluorescein fundus angiography (FFA) were performed as described previously (34).

After the mice were euthanized, representative eyeballs were carefully removed, fixed in 3.7% paraformaldehyde (PFA) and embedded in paraffin for histopathological analysis.

All animal experiments followed the guidelines of the Association for Research in Vision and Ophthalmology Statement for the Use of Animals in Ophthalmic and Vision Research. Investigators who conducted analysis were masked as to the treatment groups. All the mice were cared for by following the protocol approved by the Institutional Animal Care and Use Committee at Schepens Eye Research Institute.

Immunofluorescence

Embedded frozen fibrovascular membranes (FVMs) from patients with PDR were prepared as described previously (36). An ethical approval was obtained before the initiation of this project from the Vancouver Hospital and University of British Columbia Clinical Research Ethics Board. The University of British Columbia Clinical Research Ethics Board policies comply with the Tri Council Policy and the Good Clinical Practice Guidelines, which have their origins in the ethical principles in the Declaration of Helsinki. Written informed consent was obtained from patients.

FVMs on slides or cultured HRECs were fixed in 3.7% formaldehyde/PBS for 10 min. Subsequently, the sections or cells were preincubated with 5% normal goat serum in 0.3% Triton X-100/PBS for 20 min, incubated with primary antibodies against p110 δ (1:100 dilution) (Cat: ab2003372, Abcam, Cambridge, MA) for 1 h or a normal rabbit IgG. After 3 washes with PBS, the tissues and sections were incubated with fluorescently-labeled secondary antibodies Dylight 549 (Cat: DI-1549, Vector laboratories, Inc. Burlingame, CA) (1:300 dilution in blocking buffer) for 30 min. Following 3 washes with PBS, the slides were mounted with a mount medium containing 4',6-diamidino-2-phenylindole (DAPI) (Cat: H-1200, Vector Laboratories) and photographed under a fluorescence microscope (26,37,38).

Flow cytometry

Cultured HRECs were harvested and incubated with antibodies against VE-Cadherin, CD31 or non-immune IgG for 2 h at room temperature. After washing twice with 0.3% Triton X-100/PBS, the cells were incubated with fluorescence-labeled secondary antibodies for 1 h at room temperature. After additional triple washes with 0.3% Triton X-100/PBS, the cells were subjected to fluorescence-activated cell sorter (FACS) analysis as described previously (23).

Statistics

The data from 3 independent experiments were analyzed using an unpaired t-test between two groups, and one-way ANOVA followed by the Tukey post test among more than two groups. For animal experiments the data from at least 6 mice were used for the statistical analysis. All data were analyzed using a masked procedure. $p < 0.05$ was considered statistically significant.

Data and Resource Availability

The datasets generated during and/or analyzed during the current study are available from the corresponding author upon reasonable request. The [RESOURCE] generated during and/or analyzed during the current study is available from the corresponding author upon reasonable request.

RESULTS

p110 δ is expressed in vascular endothelial cells

The tissue distribution of p110 δ is more restricted than that of the ubiquitously-expressed other PI3K isoforms p110 α and p110 β (13). Previous studies showed that p110 δ is primarily expressed in leukocytes, but it is also found at lower levels in some non-leukocyte cell types such as ECs (22,39). As TNF α induces p110 δ expression in ECs (22) and inflammation plays an important role in diabetic retinopathy (40,41), we examined if p110 δ was expressed in ECs in FVMs from patients with PDR. Immunofluorescence revealed that p110 δ was indeed expressed in ECs of FVMs (Figure 1A-H); in addition, we found that p110 δ was also expressed in cultured human retinal microvascular endothelial cells

(HRECs) (Figure 1I-L and supplemental figure 1) and that its expression level was lower than that in mouse macrophages but much higher than that in cultured mouse cone cells (661 W) (Figure 1M-N). Specifically, p110 δ was expressed at 6.1 ± 0.7 and 22.4 ± 1.1 fold more in cultured HRECs and RAW264.7 mouse macrophages, respectively, than that in cultured 661 W cells (Figure 1N). Importantly, we discovered that high glucose (5 + 25 mM) for one week enhanced approximately 2-fold expression of p110 δ in HRECs in mRNA (Figure 1O) and protein (Figure 1P-Q). Additionally, expression of p110 δ was also detected in other vascular ECs including human umbilical vein ECs (HUVECs), porcine aortic ECs (PAECs), and human lymphatic ECs (HLECs) (Supplementary figure 2). In contrast, the expression level of p110 δ was very low in rabbit conjunctival fibroblasts (RCF) (42) and mouse 661W cone photoreceptor cells (28) (Figure 1M-N and supplementary figure 2). These results demonstrate that p110 δ is expressed in eye-related pathological and cultured ECs and high glucose promotes its expression in cultured ECs, suggesting that it plays a biological role in ECs.

p110 δ inhibition prevents Akt activation and biological responses induced by VEGF, bFGF and EGF

PI3K activation is necessary for VEGF-induced proliferation, migration and survival of cultured ECs (43). ECs express multiple PI3K isoforms, and work from other groups indicates that not all isoforms are required for the VEGF-driven responses (17). For instance, inactivation of p110 α does not block VEGF-induced proliferation and survival of vascular ECs (17). In contrast, we found that the p110 δ -selective inhibitor idelalisib at 1 μ M for 15 min completely prevented VEGF-induced Akt activation (as measured by its phosphorylation on Serine 473 (Figure 2A and D). This was also observed for Akt activation induced by bFGF (Figure 2B and D) or EGF (Figure 2C-D). In contrast, growth factor-stimulated phosphorylation of Erk (p-E202/p-Y204) was not affected (Figure 2A-C); in addition, idelalisib at 10 μ M only modestly inhibited PDGF-A-induced activation of Akt in PAECs that overexpress PDGFR α (Figure 2E), suggesting that different RTKs preferentially select different PI3K isoforms for transducing signaling to Akt and that the 10 μ M concentration of idelalisib is selective. This assumption was also supported by a

cell viability assay, which indicated that idelalisib even at higher doses was within the non-toxic range (Figure 2F). These data demonstrate that p110 δ regulates a subset of RTKs-triggered signaling pathways in HRECs, including Akt, known to play a central role in angiogenesis (44,45). In line with these observations, idelalisib was also found to blunt VEGF, bEGF or EGF promoted EC cell proliferation (Figure 3A), migration (Figure 3B-C) and tube formation (Figure 3D-E).

p110 δ depletion attenuates Akt activation, proliferation, migration and tube formation of HRECs

To complement and substantiate our data from the pharmacological approach using idelalisib, we next depleted p110 δ in HRECs using CRISPR/Cas9 technology (23,24). As shown in Figure 4A-E and supplemental figure 3, the CRISPR/Cas9 system guided by PK2-based sgRNA targeting *PIK3CD* resulted in DNA insertion and deletion in the expected genomic site, leading to depletion of p110 δ expression, without affecting expression of p110 α and p110 β (Figure 4A-C). Importantly, this p110 δ depletion attenuated Akt activation induced by VEGF (Figure 4D-F), bFGF and EGF (Figure 4G-H) and diminished cell proliferation (Figure 5A-B), migration (Figure 5C) and tube formation (Figure 5D) in these cells. Notably, idelalisib at 10 μ M did not further inhibit cell proliferation in p110 δ -depleted cells (Figure 5B), indicating that both idelalisib and PK2-sgRNA are specific for p110 δ . These results demonstrate that p110 δ plays an essential role in Akt activation and cellular responses induced by these growth factors in HRECs.

Genetic inactivation of p110 δ in mice reduces Akt activation and abnormal angiogenesis in a mouse model of oxygen-induced ischemic retinopathy

To investigate the impact of p110 δ on pathologic angiogenesis, mice with genetic inactivation of p110 δ (32) were subjected to a model of OIR (34). In the p110 δ -inactive mice, their endogenous p110 δ was replaced through germline knock-in mutation with a catalytically-inactive form of p110 δ , called p110 δ ^{D910A} (Supplemental Figure 4) (32), and their p110 δ lipid kinase activity is fully ablated, with no changes in the kinase activities of p110 α and p110 β (32).

In this mouse model of OIR, postnatal day (P) 7 mouse pups with nursing mothers are subjected to hyperoxia (75% oxygen) for 5 days, which prevents retinal vessel growth and leads to significant vessel loss in the central retina. At P12, mice were returned to room air. The switch from high oxygen to room air creates a relatively hypoxic condition which triggers both normal vessel regrowth in the avascular area of central retina and abnormal retinal angiogenesis towards to the normally avascular vitreous cavity to form unorganized, small-caliber vessels, termed preretinal tufts, which reaches a maximum at P17 (33,34).). These preretinal tufts resemble the pathologic neovascularization (NV) seen in human PDR. This OIR model has helped to lay the foundation for present clinical application of anti-VEGF therapies in patients with PDR (46-48).

Thus, OIR was induced in homozygous $p110\delta^{D910A}$ mice (further referred to as $p110\delta^{D910A/D910A}$) and their WT littermates by the techniques described above. At P17 the whole-mount retinas from the euthanized pups were stained with isolectin B4 (IB4), a mouse endothelial marker. The IB4 staining revealed a significant reduction in the area of pre-retinal tufts (pathological angiogenesis) in the eyes of $p110\delta^{D910A/D910A}$ mice compared with those of littermate WT mice, with no significant difference in the areas of vaso-obliteration between the two mouse lines (Figure 6A-C). Western blot analysis showed that there was significantly less activated Akt in the retinas from P17 $p110\delta^{D910A/D910A}$ mice as compared to those from the P17 WT mice (Figure 6D). Furthermore, ELISA analysis indicated that there was less VEGF in the vitreous from the P17 $p110\delta^{D910A/D910A}$ mice than that from the P17 WT mice experiencing OIR (Supplemental figure 5). These data demonstrate that genetic inactivation of $p110\delta$ decreases hypoxia-induced Akt activation and inhibits pathological angiogenesis but not central retinal avascular area to form neovascularization in this OIR mouse model.

Idelalisib prevents hypoxia-induced Akt activation and abnormal retinal angiogenesis in a mouse model of oxygen-induced ischemic retinopathy

To explore the impact of idelalisib on angiogenesis *in vivo*, we used a mouse model of OIR in the eye because the preretinal tufts formed in this model resemble the pathologic NV seen in human PDR (34).

We first tested the effects of an intravitreal injection of a single dose of idelalisib into P12 mice at a vitreal concentration of 8-10 μM (a dose which did not cause obvious damage to cultured HRECs (Figure 2F), followed by examination of the mouse eyes 30 days later. This was done by electroretinogram (ERG) and fundus fluorescent angiography to evaluate retinal function, and by optical coherence tomography (OCT) and histological analysis to evaluate retinal structure (Figure 7). These four assays revealed no functional or structural damage to the retina 30 days after a single injection of idelalisib.

We next examined the impact of idelalisib on pathologic angiogenesis in the mouse model of OIR (33,34). In this model as described above, at P12, when mice were returned to room air, on this day idelalisib (initial vitreal concentration of a single dose of 8-10 μM) or its vehicle (DMSO, 0.1% initial concentration) was injected into the vitreous. At P17, the whole-mount retinas from the euthanized pups were stained with IB4. Results showed a dramatic decrease in the number of preretinal tufts after treatment with idelalisib compared to vehicle (Figure 8A-C). However, idelalisib did not arrest angiogenesis from the avascular area of retinas (Figure 8A-C). In addition, idelalisib also suppressed hypoxia-induced Akt activation in the P17 retinas (Figure 8D-E). Taken together, these data show that inhibition of p110 δ prevents hypoxia-induced Akt activation and pathological angiogenesis while sparing central-avascular area's re-vascularization in this mouse model of OIR.

In summary, genetic (p110 $\delta^{\text{D910A/D910A}}$) or pharmacological (idelalisib) inactivation of p110 δ *in vivo* demonstrate that p110 δ plays an essential role in retinal pathological angiogenesis in oxygen-induced retinopathy.

Discussion

p110 δ belongs to the receptor-regulated class IA PI3K lipid kinases, which also include the p110 α and p110 β isoforms. Whereas all class I PI3Ks couple to tyrosine kinase-linked receptors, p110 β is also stimulated by G-protein-coupled receptors (12).

While TNF α induces NF κ B/p65-dependent expression of p110 δ in HUVECs, our experimental data revealed that high glucose enhances expression of p110 δ in HRECs. We hypothesize that high glucose induces NF κ B/p65 activation (49), which promotes p110 δ

expression. This hypothesis is actively being tested at present in my lab.

We herein present our findings that VEGF, bFGF and EGF are dependent on p110 δ for activating Akt in HRECs. These findings demonstrate that p110 δ can also transmit the signals from RTKs (e.g. VEGFR2, EGFR, FGFR) to activate Akt in vascular ECs. This contrasts with a previous report showing that in mouse cardiac ECs, p110 α is a predominant isoform for activating of Akt (17). This difference might be due to a different cell type using a different PI3K isoform downstream of these RTKs. In addition, by using a mouse model of OIR we found that p110 δ is required for pathological angiogenesis but not central retinal re-vascularization, while p110 α plays an essential role in developmental and tumor angiogenesis (50). The mechanism by which p110 δ is required for pathological angiogenesis but not central retinal revascularization in the OIR mouse model and why the other PI3K isoforms fail to compensate when p110 δ is antagonized, warrant further investigation.

Notably, this OIR model is not actually a model of diabetic retinopathy because diabetic retinopathy is a complex disease that involves multiple genetic and environmental inputs (e.g., high glucose) (51). However, hypoxia in this OIR model induces pathological angiogenesis (preretinal tufts), which resemble the pathologic NV seen in human PDR. Therefore, this OIR model partially mimics the pathological angiogenesis in the patients with PDR (46-48).

Idelalisib (also known as GS-1101, CAL-101 or Zydelig) is a selective inhibitor of p110 δ , approved by the United States Food and Drug Administration for the treatment of hematological malignancies (52). Our data provide a potentially alternative approach to treating the patients with neovascular eye diseases who are not completely responsive to the current anti-VEGF treatment. Mainly due to its immunomodulatory effects, systemic exposure to idelalisib comes with warnings of possible toxicities that are serious and even fatal, the use of idelalisib to treat eyes might result in potential harmful side effects (53). However, this toxicity might not be observed upon intravitreal administration to treat angiogenesis-related eye diseases. With regards to the possible risk to the retina and visual function, our results showed that a single intravitreal injection of idelalisib did not cause deleterious effects on retinal structure and function within one month (Figure 7). However, if multiple intravitreal injections need to achieve suppression of pathological retinal

neovascularization in clinical settings, retinal structure and function will have to be closely evaluated and monitored further.

In contrast to mice lacking p110 α or β which show full or partial embryonic death (54,55), our experiments confirmed that mice with inactive p110 δ are fertile, born at normal Mendelian ratios without gross anatomical or behavioral abnormalities (32), indicating that p110 δ is not critical for development and physiological angiogenesis. However, our data clearly show that these mice display reduced pathological retinal angiogenesis in an OIR model (Figure 6), demonstrating that p110 δ activity contributes to pathological retinal angiogenesis. This is consistent with another report that p110 δ inactivation does not affect normal vascular development (17). Because mice with inactive p110 δ mice are viable, the other PI3K isoforms may replace p110 δ activity during development and physiological angiogenesis, indicating that p110 δ contributes exclusively to pathological retinal angiogenesis.

Notably, leukocytes (e.g. macrophages), in which p110 δ is highly expressed, also play an important role in angiogenesis (56), so whether p110 δ plays an essential role in pathogenesis via ECs *in vivo* needs further investigation.

In conclusion, our findings establish a conceptual foundation for developing a p110 δ -targeted approach to prevent and treat retinal angiogenesis such as those seen in PDR. Especially, the pharmacological (idelalisib) has great potential for development as alternatives for those patients who sub-optimally respond to current anti-VEGF drugs.

Finance Disclosure: This work was supported by the National Eye Institute of the National Institutes of Health under Award Number R01EY012509 (to H.L) and Core Grant P30EY003790, Global Ophthalmology Award Program (to H.L), and Research to Prevent Blindness (to H.L); China Scholarship Council (to W.W.) and Central South University student innovation project 2016zzts148 (to W.W.). National Natural Science Foundation of China (81900893) to W.W, the Science and Technology Plan Project of Hunan Province (2019RS2011) to W.W. No funding bodies had any role in study design, data collection and analysis, decision to publish, or preparation of the manuscript.

Competing financial interests: There is a pending patent application related to this work (to H.L.) at Schepens Eye Research Institute of Massachusetts Eye and Ear. B.V. is a consultant for Karus Therapeutics (Oxford, UK), iOnctura (Geneva, Switzerland) and Venthera (Palo Alto, US) and has received speaker fees for Gilead. Other authors declare that they do not have any competing financial interests.

Acknowledgements: Dr. Hetian Lei is the guarantor of this work, and has full access to all the data in the study and takes responsibility for the integrity of the data and the accuracy of the data analysis. We thank Dr. Patricia A. D'Amore for revising the manuscript and Dr. Michele Leblanc for analysis of neovascularization in the whole mount retinal staining.

Author contributions: W.W., G.Z., H.H., X.H. and H.J. performed the experiments and analyzed the results; S.M. provided reagents and critically revised the manuscript; J.C. and J.M. provided patient samples and revised the manuscript; B.V. provided reagents, helped to interpret the data and edited the manuscript; A.K. conceived the experiments and revised the manuscript; X.X., J.L, and J.W conceived the experiments and revised the manuscript. H.L. conceived the experiments, analyzed the data and wrote the manuscript.

References

1. Duh, E. J., Sun, J. K., and Stitt, A. W. (2017) Diabetic retinopathy: current understanding, mechanisms, and treatment strategies. *JCI Insight* **2**
2. Williams, R., Airey, M., Baxter, H., Forrester, J., Kennedy-Martin, T., and Girach, A. (2004) Epidemiology of diabetic retinopathy and macular oedema: a systematic review. *Eye (Lond)* **18**, 963-983
3. Cross, M. J., and Claesson-Welsh, L. (2001) FGF and VEGF function in angiogenesis: signalling pathways, biological responses and therapeutic inhibition. *Trends Pharmacol Sci* **22**, 201-207
4. Ellis, L. M. (2004) Epidermal growth factor receptor in tumor angiogenesis. *Hematol Oncol Clin North Am* **18**, 1007-1021, viii
5. Senger, D. R., Galli, S. J., Dvorak, A. M., Perruzzi, C. A., Harvey, V. S., and Dvorak, H. F. (1983) Tumor cells secrete a vascular permeability factor that promotes accumulation of ascites fluid. *Science* **219**, 983-985
6. Mintz-Hittner, H. A., Kennedy, K. A., Chuang, A. Z., and Group, B.-R. C. (2011) Efficacy of intravitreal bevacizumab for stage 3+ retinopathy of prematurity. *N Engl J Med* **364**, 603-615

7. Chakravarthy, U., Harding, S. P., Rogers, C. A., Downes, S. M., Lotery, A. J., Culliford, L. A., Reeves, B. C., and investigators, I. s. (2013) Alternative treatments to inhibit VEGF in age-related choroidal neovascularisation: 2-year findings of the IVAN randomised controlled trial. *Lancet* **382**, 1258-1267
8. Fogli, S., Del Re, M., Rofi, E., Posarelli, C., Figus, M., and Danesi, R. (2018) Clinical pharmacology of intravitreal anti-VEGF drugs. *Eye (Lond)* **32**, 1010-1020
9. Suzuki, M., Nagai, N., Izumi-Nagai, K., Shinoda, H., Koto, T., Uchida, A., Mochimaru, H., Yuki, K., Sasaki, M., Tsubota, K., and Ozawa, Y. (2014) Predictive factors for non-response to intravitreal ranibizumab treatment in age-related macular degeneration. *Br J Ophthalmol* **98**, 1186-1191
10. Vanhaesebroeck, B., Stephens, L., and Hawkins, P. (2012) PI3K signalling: the path to discovery and understanding. *Nature reviews. Molecular cell biology* **13**, 195-203
11. Graupera, M., and Potente, M. (2013) Regulation of angiogenesis by PI3K signaling networks. *Experimental cell research* **319**, 1348-1355
12. Bilanges, B., Posor, Y., and Vanhaesebroeck, B. (2019) PI3K isoforms in cell signalling and vesicle trafficking. *Nature reviews. Molecular cell biology*
13. Vanhaesebroeck, B., Welham, M. J., Kotani, K., Stein, R., Warne, P. H., Zvelebil, M. J., Higashi, K., Volinia, S., Downward, J., and Waterfield, M. D. (1997) P110delta, a novel phosphoinositide 3-kinase in leukocytes. *Proc Natl Acad Sci U S A* **94**, 4330-4335
14. Okkenhaug, K. (2013) Signaling by the phosphoinositide 3-kinase family in immune cells. *Annual review of immunology* **31**, 675-704
15. Ali, K., Soond, D. R., Pineiro, R., Hagemann, T., Pearce, W., Lim, E. L., Bouabe, H., Scudamore, C. L., Hancox, T., Maecker, H., Friedman, L., Turner, M., Okkenhaug, K., and Vanhaesebroeck, B. (2014) Inactivation of PI(3)K p110delta breaks regulatory T-cell-mediated immune tolerance to cancer. *Nature* **510**, 407-411
16. Chellappa, S., Kushekhar, K., Munthe, L. A., Tjonnfjord, G. E., Aandahl, E. M., Okkenhaug, K., and Tasken, K. (2019) The PI3K p110delta Isoform Inhibitor Idelalisib Preferentially Inhibits Human Regulatory T Cell Function. *Journal of immunology* **202**, 1397-1405
17. Graupera, M., Guillermet-Guibert, J., Foukas, L. C., Phng, L. K., Cain, R. J., Salpekar, A., Pearce, W., Meek, S., Millan, J., Cutillas, P. R., Smith, A. J., Ridley, A. J., Ruhrberg, C., Gerhardt, H., and Vanhaesebroeck, B. (2008) Angiogenesis selectively requires the p110alpha isoform of PI3K to control endothelial cell migration. *Nature* **453**, 662-666
18. Haddad, G., Zhabyeyev, P., Farhan, M., Zhu, L. F., Kassiri, Z., Rayner, D. C., Vanhaesebroeck, B., Oudit, G. Y., and Murray, A. G. (2014) Phosphoinositide 3-kinase beta mediates microvascular endothelial repair of thrombotic microangiopathy. *Blood* **124**, 2142-2149
19. Vanhaesebroeck, B., Whitehead, M. A., and Pineiro, R. (2016) Molecules in medicine mini-review: isoforms of PI3K in biology and disease. *J Mol Med (Berl)* **94**, 5-11

20. Puri, K. D., and Gold, M. R. (2012) Selective inhibitors of phosphoinositide 3-kinase delta: modulators of B-cell function with potential for treating autoimmune inflammatory diseases and B-cell malignancies. *Frontiers in immunology* **3**, 256
21. Bartok, B., Hammaker, D., and Firestein, G. S. (2014) Phosphoinositide 3-kinase delta regulates migration and invasion of synoviocytes in rheumatoid arthritis. *Journal of immunology* **192**, 2063-2070
22. Whitehead, M. A., Bombardieri, M., Pitzalis, C., and Vanhaesebroeck, B. (2012) Isoform-selective induction of human p110delta PI3K expression by TNFalpha: identification of a new and inducible PIK3CD promoter. *Biochem J* **443**, 857-867
23. Huang, X., Zhou, G., Wu, W., Ma, G., D'Amore, P. A., Mukai, S., and Lei, H. (2017) Editing VEGFR2 Blocks VEGF-Induced Activation of Akt and Tube Formation. *Invest Ophthalmol Vis Sci* **58**, 1228-1236
24. Swiech, L., Heidenreich, M., Banerjee, A., Habib, N., Li, Y., Trombetta, J., Sur, M., and Zhang, F. (2015) In vivo interrogation of gene function in the mammalian brain using CRISPR-Cas9. *Nature biotechnology* **33**, 102-106
25. Sanjana, N. E., Shalem, O., and Zhang, F. (2014) Improved vectors and genome-wide libraries for CRISPR screening. *Nat Methods* **11**, 783-784
26. Lei, H., Romeo, G., and Kazlauskas, A. (2004) Heat shock protein 90alpha-dependent translocation of annexin II to the surface of endothelial cells modulates plasmin activity in the diabetic rat aorta. *Circ Res* **94**, 902-909
27. Lei, H., Qian, C. X., Lei, J., Haddock, L. J., Mukai, S., and Kazlauskas, A. (2015) RasGAP Promotes Autophagy and Thereby Suppresses Platelet-Derived Growth Factor Receptor-Mediated Signaling Events, Cellular Responses, and Pathology. *Mol Cell Biol* **35**, 1673-1685
28. Tan, E., Ding, X. Q., Saadi, A., Agarwal, N., Naash, M. I., and Al-Ubaidi, M. R. (2004) Expression of cone-photoreceptor-specific antigens in a cell line derived from retinal tumors in transgenic mice. *Invest Ophthalmol Vis Sci* **45**, 764-768
29. Lei, H., Velez, G., Hovland, P., Hirose, T., Gilbertson, D., and Kazlauskas, A. (2009) Growth factors outside the PDGF family drive experimental PVR. *Invest Ophthalmol Vis Sci* **50**, 3394-3403
30. Zhou, G., Duan, Y., Ma, G., Wu, W., Hu, Z., Chen, N., Chee, Y., Cui, J., Samad, A., Matsubara, J. A., Mukai, S., D'Amore, P. A., and Lei, H. (2017) Introduction of the MDM2 T309G Mutation in Primary Human Retinal Epithelial Cells Enhances Experimental Proliferative Vitreoretinopathy. *Invest Ophthalmol Vis Sci* **58**, 5361-5367
31. Riss, T. L., Moravec, R. A., Niles, A. L., Duellman, S., Benink, H. A., Worzella, T. J., and Minor, L. (2004) Cell Viability Assays. in *Assay Guidance Manual* (Sittampalam, G. S., Coussens, N. P., Brimacombe, K., Grossman, A., Arkin, M., Auld, D., Austin, C., Baell, J., Bejcek, B., Caaveiro, J. M. M., Chung, T. D. Y., Dahlin, J. L., Devanaryan, V., Foley, T. L., Glicksman, M., Hall, M. D., Haas, J. V., Inglese, J., Iversen, P. W., Kahl, S. D., Kales, S. C., Lal-Nag, M., Li, Z., McGee, J., McManus, O., Riss, T., Trask, O. J., Jr., Weidner, J. R., Wildey, M. J., Xia, M., and Xu, X. eds.), Bethesda (MD). pp

32. Okkenhaug, K., Bilancio, A., Farjot, G., Priddle, H., Sancho, S., Peskett, E., Pearce, W., Meek, S. E., Salpekar, A., Waterfield, M. D., Smith, A. J., and Vanhaesebroeck, B. (2002) Impaired B and T cell antigen receptor signaling in p110delta PI 3-kinase mutant mice. *Science* **297**, 1031-1034
33. Connor, K. M., Krahn, N. M., Dennison, R. J., Aderman, C. M., Chen, J., Guerin, K. I., Sapieha, P., Stahl, A., Willett, K. L., and Smith, L. E. (2009) Quantification of oxygen-induced retinopathy in the mouse: a model of vessel loss, vessel regrowth and pathological angiogenesis. *Nat Protoc* **4**, 1565-1573
34. Huang, X., Zhou, G., Wu, W., Duan, Y., Ma, G., Song, J., Xiao, R., Vandenberghe, L., Zhang, F., D'Amore, P. A., and Lei, H. (2017) Genome editing abrogates angiogenesis in vivo. *Nature communications* **8**, 112
35. Longchamp, A., Mirabella, T., Arduini, A., MacArthur, M. R., Das, A., Trevino-Villarreal, J. H., Hine, C., Ben-Sahra, I., Knudsen, N. H., Brace, L. E., Reynolds, J., Mejia, P., Tao, M., Sharma, G., Wang, R., Corpataux, J. M., Haefliger, J. A., Ahn, K. H., Lee, C. H., Manning, B. D., Sinclair, D. A., Chen, C. S., Ozaki, C. K., and Mitchell, J. R. (2018) Amino Acid Restriction Triggers Angiogenesis via GCN2/ATF4 Regulation of VEGF and H2S Production. *Cell* **173**, 117-129 e114
36. Cui, J., Lei, H., Samad, A., Basavanthappa, S., Maberley, D., Matsubara, J., and Kazlauskas, A. (2009) PDGF receptors are activated in human epiretinal membranes. *Exp Eye Res* **88**, 438-444
37. Lei, H., Rheume, M. A., Cui, J., Mukai, S., Maberley, D., Samad, A., Matsubara, J., and Kazlauskas, A. (2012) A novel function of p53: a gatekeeper of retinal detachment. *Am J Pathol* **181**, 866-874
38. Ma, G., Duan, Y., Huang, X., Qian, C. X., Chee, Y., Mukai, S., Cui, J., Samad, A., Matsubara, J. A., Kazlauskas, A., D'Amore, P. A., Gu, S., and Lei, H. (2016) Prevention of Proliferative Vitreoretinopathy by Suppression of Phosphatidylinositol 5-Phosphate 4-Kinases. *Invest Ophthalmol Vis Sci* **57**, 3935-3943
39. Puri, K. D., Doggett, T. A., Douangpanya, J., Hou, Y., Tino, W. T., Wilson, T., Graf, T., Clayton, E., Turner, M., Hayflick, J. S., and Diacovo, T. G. (2004) Mechanisms and implications of phosphoinositide 3-kinase delta in promoting neutrophil trafficking into inflamed tissue. *Blood* **103**, 3448-3456
40. Tang, J., and Kern, T. S. (2011) Inflammation in diabetic retinopathy. *Prog Retin Eye Res* **30**, 343-358
41. Rubsam, A., Parikh, S., and Fort, P. E. (2018) Role of Inflammation in Diabetic Retinopathy. *Int J Mol Sci* **19**
42. Arnaoutova, I., and Kleinman, H. K. (2010) In vitro angiogenesis: endothelial cell tube formation on gelled basement membrane extract. *Nat Protoc* **5**, 628-635
43. Gerber, H. P., McMurtrey, A., Kowalski, J., Yan, M., Keyt, B. A., Dixit, V., and Ferrara, N. (1998) Vascular endothelial growth factor regulates endothelial cell survival through the phosphatidylinositol 3'-kinase/Akt signal transduction pathway. Requirement for Flk-1/KDR activation. *J Biol Chem* **273**, 30336-30343
44. Dimmeler, S., and Zeiher, A. M. (2000) Akt takes center stage in angiogenesis signaling. *Circ Res* **86**, 4-5

45. Manning, B. D., and Toker, A. (2017) AKT/PKB Signaling: Navigating the Network. *Cell* **169**, 381-405
46. Chen, J., Connor, K. M., Aderman, C. M., Willett, K. L., Aspegren, O. P., and Smith, L. E. (2009) Suppression of retinal neovascularization by erythropoietin siRNA in a mouse model of proliferative retinopathy. *Invest Ophthalmol Vis Sci* **50**, 1329-1335
47. Nagai, N., Ju, M., Izumi-Nagai, K., Robbie, S. J., Bainbridge, J. W., Gale, D. C., Pierre, E., Krauss, A. H., Adamson, P., Shima, D. T., and Ng, Y. S. (2015) Novel CCR3 Antagonists Are Effective Mono- and Combination Inhibitors of Choroidal Neovascular Growth and Vascular Permeability. *Am J Pathol* **185**, 2534-2549
48. Stahl, A., Connor, K. M., Sapienza, P., Chen, J., Dennison, R. J., Krah, N. M., Seaward, M. R., Willett, K. L., Aderman, C. M., Guerin, K. I., Hua, J., Lofqvist, C., Hellstrom, A., and Smith, L. E. (2010) The mouse retina as an angiogenesis model. *Invest Ophthalmol Vis Sci* **51**, 2813-2826
49. Ramana, K. V., Friedrich, B., Srivastava, S., Bhatnagar, A., and Srivastava, S. K. (2004) Activation of nuclear factor-kappaB by hyperglycemia in vascular smooth muscle cells is regulated by aldose reductase. *Diabetes* **53**, 2910-2920
50. Soler, A., Serra, H., Pearce, W., Angulo, A., Guillermet-Guibert, J., Friedman, L. S., Vinals, F., Gerhardt, H., Casanovas, O., Graupera, M., and Vanhaesebroeck, B. (2013) Inhibition of the p110alpha isoform of PI 3-kinase stimulates nonfunctional tumor angiogenesis. *The Journal of experimental medicine* **210**, 1937-1945
51. Olivares, A. M., Althoff, K., Chen, G. F., Wu, S., Morrisson, M. A., DeAngelis, M. M., and Haider, N. (2017) Animal Models of Diabetic Retinopathy. *Curr Diab Rep* **17**, 93
52. Gopal, A. K., Kahl, B. S., de Vos, S., Wagner-Johnston, N. D., Schuster, S. J., Jurczak, W. J., Flinn, I. W., Flowers, C. R., Martin, P., Viardot, A., Blum, K. A., Goy, A. H., Davies, A. J., Zinzani, P. L., Dreyling, M., Johnson, D., Miller, L. L., Holes, L., Li, D., Dansey, R. D., Godfrey, W. R., and Salles, G. A. (2014) PI3Kdelta inhibition by idelalisib in patients with relapsed indolent lymphoma. *N Engl J Med* **370**, 1008-1018
53. Tang, L. A., Dixon, B. N., Maples, K. T., Poppiti, K. M., and Peterson, T. J. (2018) Current and Investigational Agents Targeting the Phosphoinositide 3-Kinase Pathway. *Pharmacotherapy* **38**, 1058-1067
54. Foukas, L. C., Claret, M., Pearce, W., Okkenhaug, K., Meek, S., Peskett, E., Sancho, S., Smith, A. J., Withers, D. J., and Vanhaesebroeck, B. (2006) Critical role for the p110alpha phosphoinositide-3-OH kinase in growth and metabolic regulation. *Nature* **441**, 366-370
55. Guillermet-Guibert, J., Smith, L. B., Halet, G., Whitehead, M. A., Pearce, W., Rebourcet, D., Leon, K., Crepieux, P., Nock, G., Stromstedt, M., Enerback, M., Chelala, C., Graupera, M., Carroll, J., Cosulich, S., Saunders, P. T., Huhtaniemi, I., and Vanhaesebroeck, B. (2015) Novel Role for p110beta PI 3-Kinase in Male Fertility through Regulation of Androgen Receptor Activity in Sertoli Cells. *PLoS Genet* **11**, e1005304

56. Jetten, N., Verbruggen, S., Gijbels, M. J., Post, M. J., De Winther, M. P., and Donners, M. M. (2014) Anti-inflammatory M2, but not pro-inflammatory M1 macrophages promote angiogenesis in vivo. *Angiogenesis* **17**, 109-118

Figure legends

Figure 1. High glucose induced p110 δ expression in vascular ECs

A-H. FVMs from PDR patients on slides were subjected to immunofluorescence analysis using antibodies against p110 δ and CD31 (A-D) or control antibodies (rabbit and mouse) IgG (E-H). Red and green signals indicate expression of p110 δ and CD31, respectively, in comparison to the negative non-immune IgG stained control. Blue signals are from nucleus staining with DAPI. This is a representative of 3 independent experiments using different sample sources (FVMs from 3 PDR patients). The images were taken under immunofluorescence microscope. Scale bar: 200 μ m.

I-L. HRECs at passage 6 in a slide chamber were subjected to immunofluorescence analysis using antibodies against p110 δ and CD31 as performed in A-H. Scale bar: 20 μ m.

M-N. Lysates of RAW264.7 (RAW), HRECs and 661W cells were subjected to western blot analysis using indicated antibodies. The intensity of the p110 δ bands was firstly normalized to that of the corresponding β -Actin bands. Each plot in N indicates mean \pm standard deviation (SD) of 3 independent experiments (folds). **** indicates significant difference ($p < 0.001$) between two compared groups using one-way ANOVA followed by a Tukey post test.

O-Q. HRECs exposed to normal D-glucose (N, 5 mM), L-glucose (L, 5 mM D-glucose + 25 mM L-glucose) and high D-glucose (D, 5 mM original D-glucose + 25 mM additional D-glucose) for one week were subjected to quantitative PCR and western blot for analysis of mRNA and protein expression. The intensity quantitation of protein expression was performed in P-Q. Each plot in O and Q indicates mean \pm SD of 3 independent experiments (folds). *** and **** indicate significant difference ($p < 0.001$, and $p < 0.0001$, respectively) using one-way ANOVA followed by the Tukey post test; ns: not significant.

Figure 2. Inhibition of PI3K δ prevents Akt activation induced by VEGF, bFGF or EGF

A-D. When HRECs reached about 90% confluence, the cultured medium was replaced with the endothelial basal medium without growth factors and continuously cultured for 8

h. Then, these cells were treated with idelalisib at the indicated concentrations or its vehicle in addition to VEGF-A (A), bFGF (B) or EGF (C) (10 ng/ml). V: vehicle (0.1% DMSO). After this treatment lasted for 15 min, the cells were lysed. Their lysates were subjected to a western blot analysis using the indicated antibodies. A representative of 3 independent experiments is shown. Each plot in D indicates the mean \pm SD of 3 independent experiments (folds). ** and **** indicate significant difference ($p < 0.01$, 0.0001) using one-way ANOVA followed by the Tukey post test.

E. Serum-deprived PAECs, which overexpressed PDGFR α , were treated with idelalisib at the indicated concentrations or its vehicle in addition to PDGF-A (10 ng/ml) for 15 min. Their lysates were subjected to western blot analysis using indicated antibodies. This is representative of three independent experiments.

F. HRECs treated with idelalisib as indicated concentrations and time course were subjected to a MTT assay. IC₅₀ of idelalisib to HRECs was 15 μ M at 72 h.

Figure 3. Inhibition of PI3K δ inhibits cell proliferation, migration and tube formation induced by VEGF, bFGF or EGF

A. HRECs were seeded into 24-well plates at a density of 30,000 cells/well in endothelial growth medium. After attaching the plates, the cells were starved of growth factors for 8 h and then treated with idelalisib (10 μ M), vehicle (V) with or without VEGF, bFGF or EGF (20 ng/ml). After 24 h, the cells were trypsin detached and then counted in a hemocytometer under a light microscope.

B-C. When HRECs reached confluence in 48-well plates and starved of growth factors for 8 h, a wound was created by scraping the cell monolayer with a sterile pipette tip. The cells were washed twice to remove detached cells and then treated with idelalisib (10 μ M), its vehicle (V), supplemented with or without VEGF, bFGF or EGF (20 ng/ml). At 18 h post wounding, the wound was photographed under a microscope. Scale bar: 400 μ m.

D-E. After polymerization of the collagen gel, HRECs (4.0×10^4) were seeded in each well in the culture medium overnight. After addition of second layer of gel, cells were treated with idelalisib (10 μ M), its vehicle (V) supplemented with VEGF, bFGF or EGF (20 ng/ml). 6 h later, each well was photographed under a microscope. Scale bar: 1000 μ m.

Each plot in **A**, **C** and **E** indicates the mean \pm SD of 3 independent experiments. *** and **** denote significant difference ($p < 0.001$ and 0.0001) using one-way ANOVA followed by the Tukey post test.

Figure 4. Depletion of p110 δ attenuates Akt activation induced by VEGF, bFGF, or EGF

A. Schematic of the human genomic *PIK3CD* locus. One target for generating its sgRNA was selected at the human genomic *PIK3CD* exon 4 and named as PK2 (green line). The protospacer-adjacent motif (PAM) sequences are marked in short thick blue lines.

B. Genomic DNA isolated from HRECs with CRISPR/Cas9 targeting to p110 δ by sgRNA-PK2 or control by sgRNA-*lacZ* were used to PCR amplify the DNA fragments around sgRNA-PK2 protospacer with primers (P24F1, 5'-GGGAGGTTTGGACCCCCAG-3'); P24R1 (reverse: ACCTTTGCCGATGAGGAGGC for Sanger DNA sequencing).

C. Lysates of HRECs expressing sgRNA-*lacZ* or PK2/Cas9 were subjected to western blot analysis using indicated antibodies. This is representative of three independent experiments.

D-H. The characterized HRECs in **B** were cultured to 90% confluence and then starved of growth factors for 8 h. Subsequently, these cells were treated with VEGF, bFGF and EGF (10 ng/ml) for 15 min and their clarified lysates subjected to western blot analysis using the indicated antibodies. A representative of 3 independent experiments is shown. The intensity of the bands from 3 experiments was quantified as dot plots. Each plot in **F**, **F** and **H** indicates the mean \pm SD of 3 independent experiments. *, *** and **** indicate significant difference ($p < 0.05$, 0.001 and 0.0001) using one-way ANOVA followed by the Tukey post hoc-test.

Figure 5. Depletion of p110 δ attenuates cell proliferation, migration and tube formation

A-B. HRECs expressing *lacZ* or PK2-sgRNA/Cas9 were seeded into 24-well plates at a density of 30,000 cells/well in an endothelial growth medium kit with or without treatment with idelalisib (Idel, 10 μ M). After 24 h, the cells were trypsin-detached and counted in a

hemocytometer under a light microscope. The mean \pm SD of 3 independent experiments is shown.

C. When HRECs reached 90% confluence in 48-well plates, a wound was created by scraping the cell monolayer with a 200 μ l-sterile pipette tip. At 18 h post wounding, the wound was photographed under a microscope. Shown is a representative of 3 independent experiments. Scale bar: 400 μ m.

E. A collagen gel mixture was added to a 96-well plate. After polymerization, HRECs (4.0×10^4) were seeded in each well with their culture medium maintained at a 37°C incubator. The next day, the top gel was added. Six hours later, each well was photographed under a microscope. Shown is a representative of 3 independent experiments. Scale bar: 400 μ m.

Each plot in this figure indicates mean \pm SD of 3 independent experiments. ** and *** denote significant difference ($p < 0.01$ and 0.001 , respectively) in A, C and D between the two compared groups using unpaired t test and in B using one-way ANOVA followed by the Tukey post hoc-test. NS: not significant.

Figure 6. Genetic inactivation of p110 δ attenuates Akt activation and aberrant angiogenesis in a mouse model of OIR

A-C. Litters of WT and p110 $\delta^{D910A/D910A}$ (D910A) mice were exposed to 75% oxygen from P7 to P12 for 5 days, and then returned to room air. At P17, whole-mount-retinas were stained with IB4 (n = 6) (**A**). Analysis of pathological angiogenesis (Tufts) (**B**) and avascular (**C**) areas from the IB4-stained retinas. **** indicates significant difference ($p < 0.0001$) between the two compared groups (6 retinas per group) using an unpaired t-test. NS: not significant.

D. The clarified lysates of the retinas (one retina per lane) from P17 pups having experienced the OIR model were subjected to western blot using the indicated antibodies. Each plot indicates the mean \pm SD of 3 independent experiments; *** indicates significant difference ($p < 0.001$) using an unpaired t-test.

Fig. 7. Evaluation of Idelalisib toxicity to mouse eyes

Idelalisib was intravitreally injected into the mouse eyes on P12 to achieve a final vitreal concentration of approximately 10 μM . This day was considered day 0. On day 30, the mouse eyes were examined by ERG (dark adaption) (A), OCT (B), fluorescein fundus angiography (FFA) (C), and histological analysis (D). Representative data are presented in each panel for the indicated analysis. R: right eye, L: left eye, INL: inner nuclear layer, ONL: outer nuclear layer, H & E: hematoxylin and eosin stain. Scale bar: 200 μm .

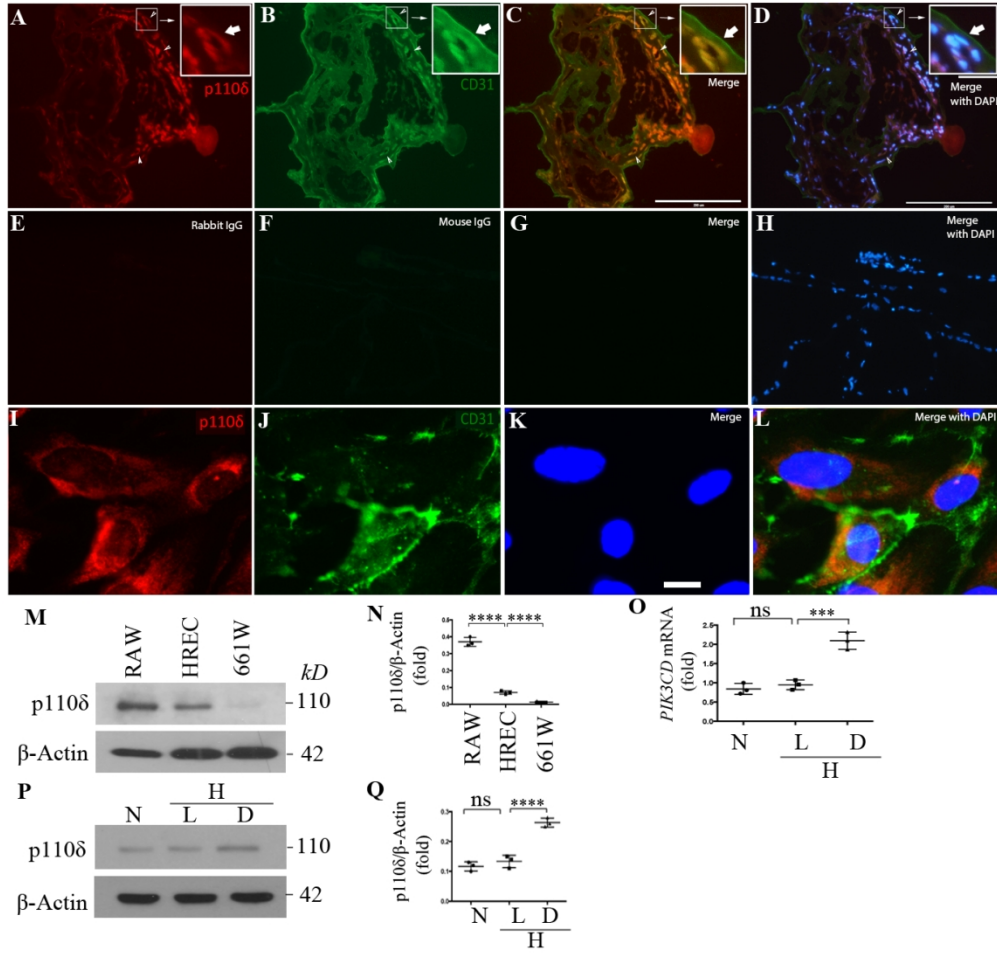
Figure 8. Inhibition of p110 δ suppresses Akt activation and pathological angiogenesis in a mouse model of OIR

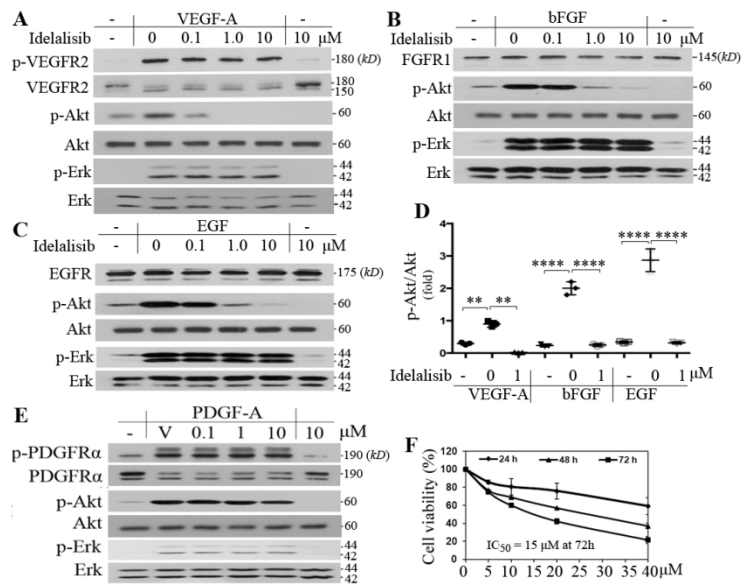
Litters of P12 mice that had been exposed to 75% oxygen for 5 days were injected intravitreally with idelalisib (Idel, final vitreal concentration of approximately 10 μM) or its vehicle (V: 0.1% DMSO) and then stayed in room air for 5 days.

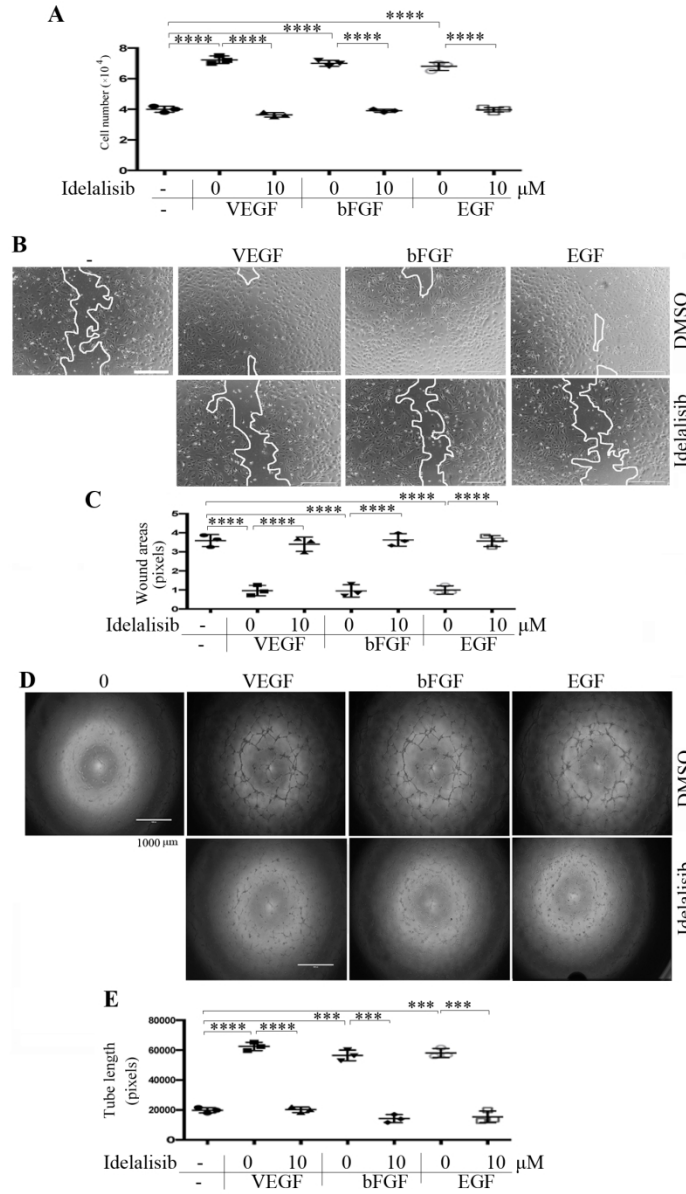
A-C. At P17, whole-mount-retinas were stained with IB4 (A). Analysis of neovascularization (NV) areas (tufts) from the IB4-stained retinas (n = 6) (B) and avascular area (n = 6) (C).

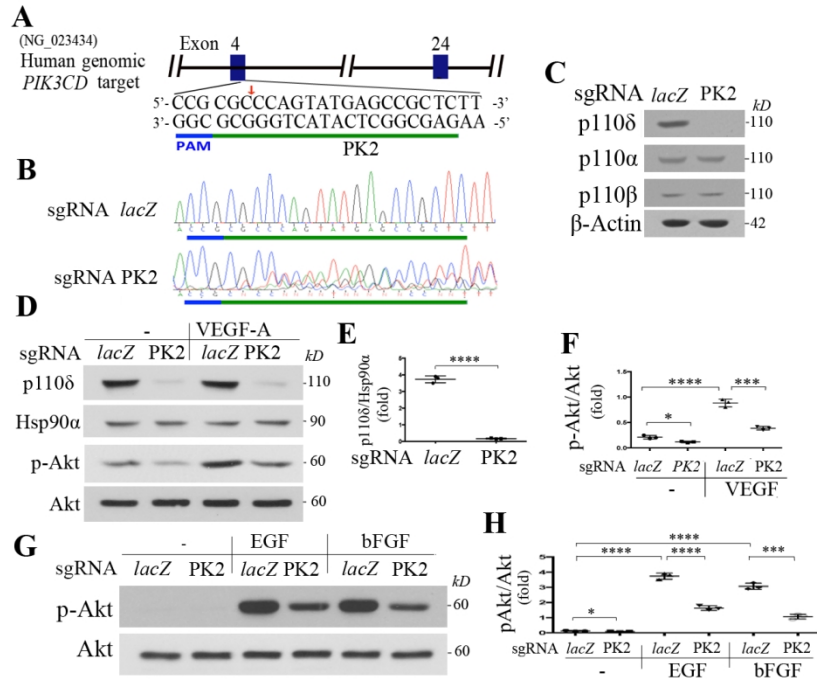
D-E. Total lysates from retinas (one retina per lane) were subjected to western blot analysis using the indicated antibodies. N: retinas from P17 mice without experiencing 75% high oxygen.

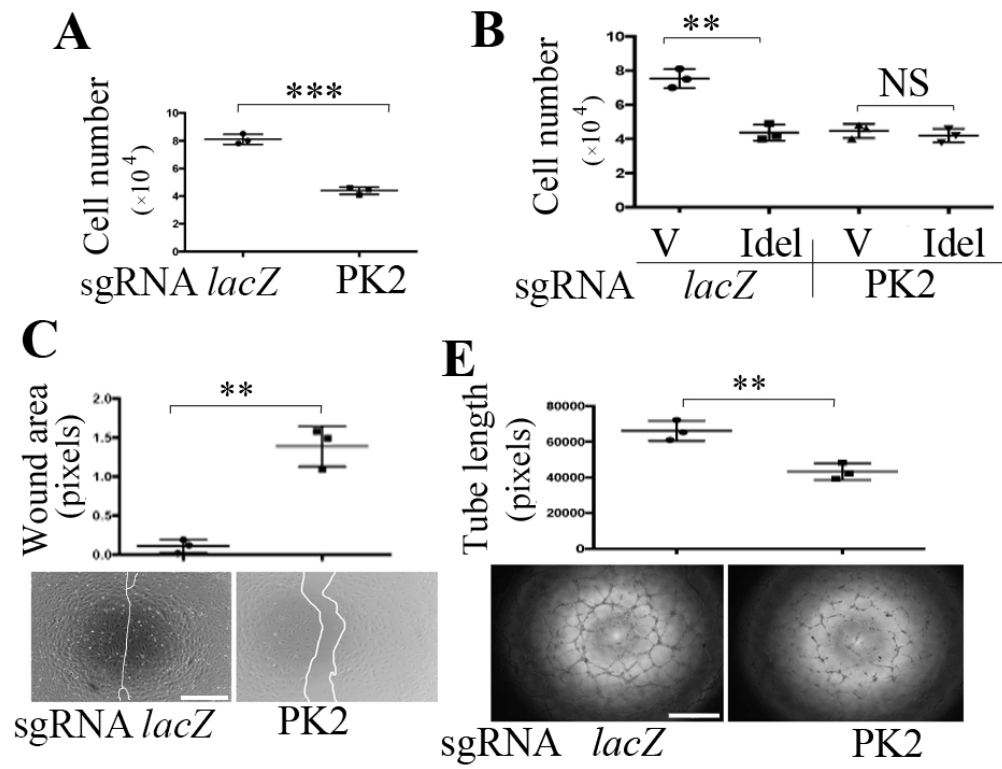
Each plot in this figure indicates the mean \pm SD of 3 independent experiments (folds). * and **** indicate significant difference ($p < 0.05$, 0.0001) between two compared groups using an unpaired t-test. ns: not significant.

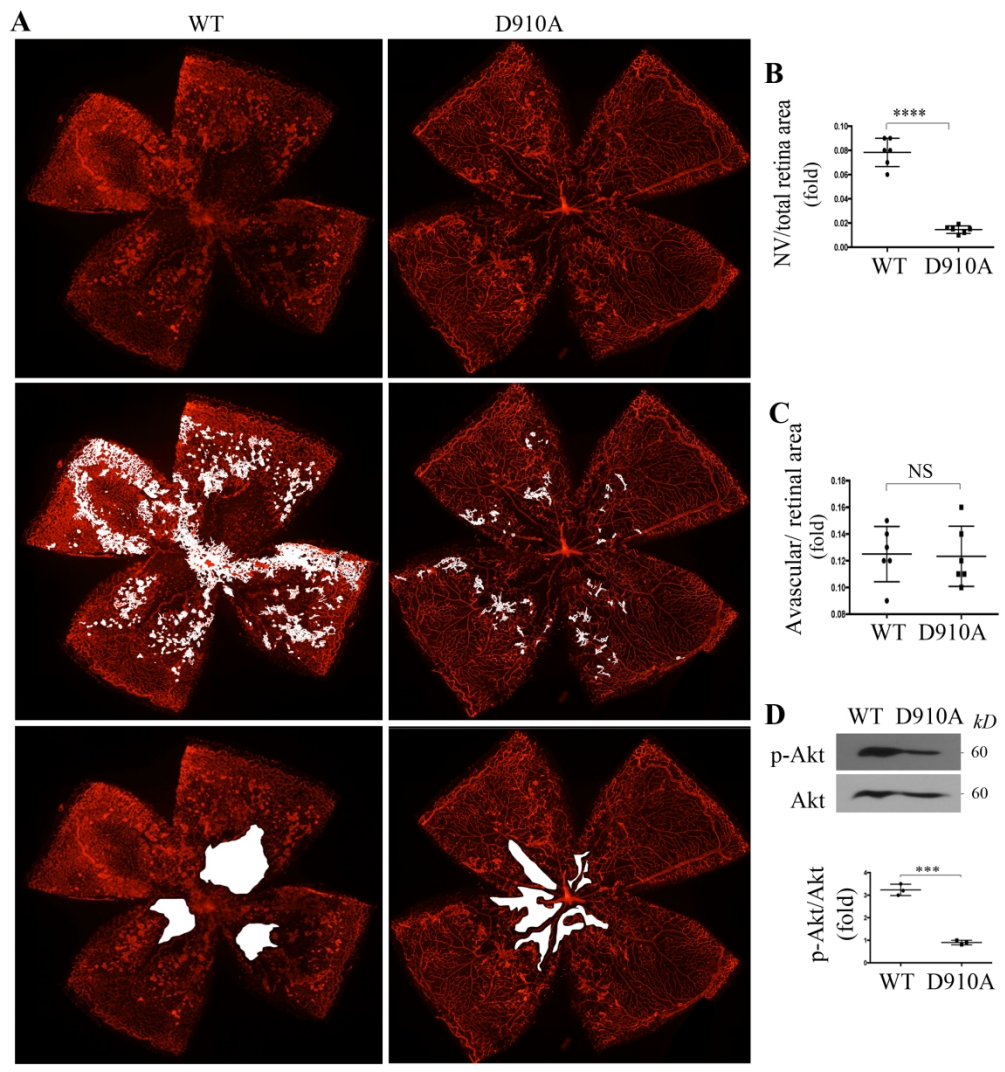


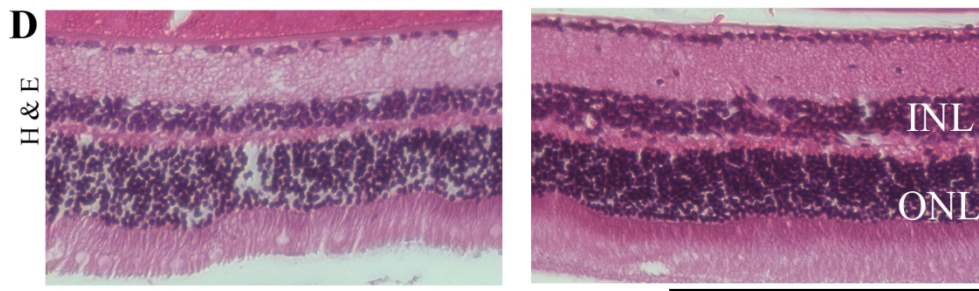
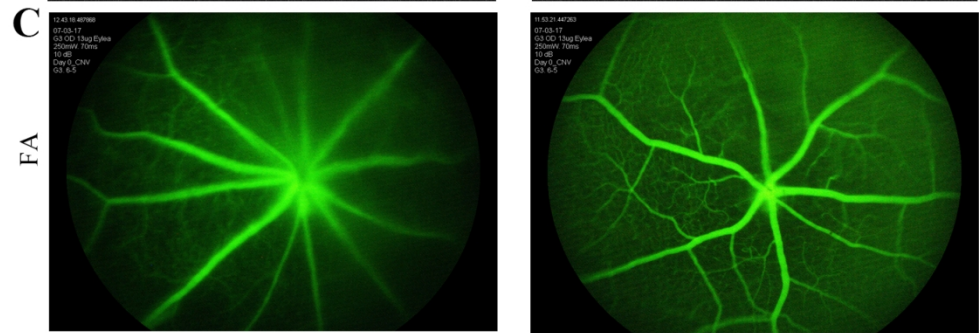
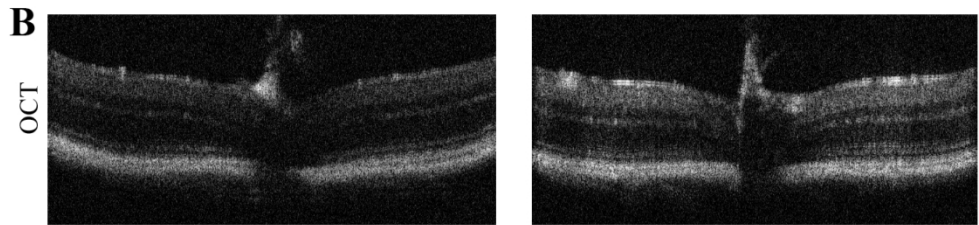
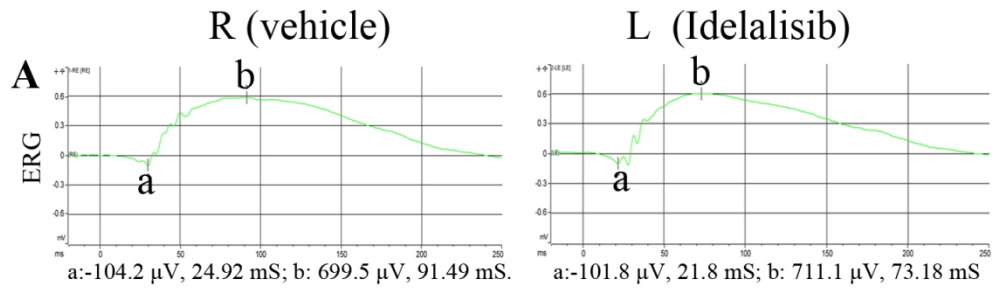


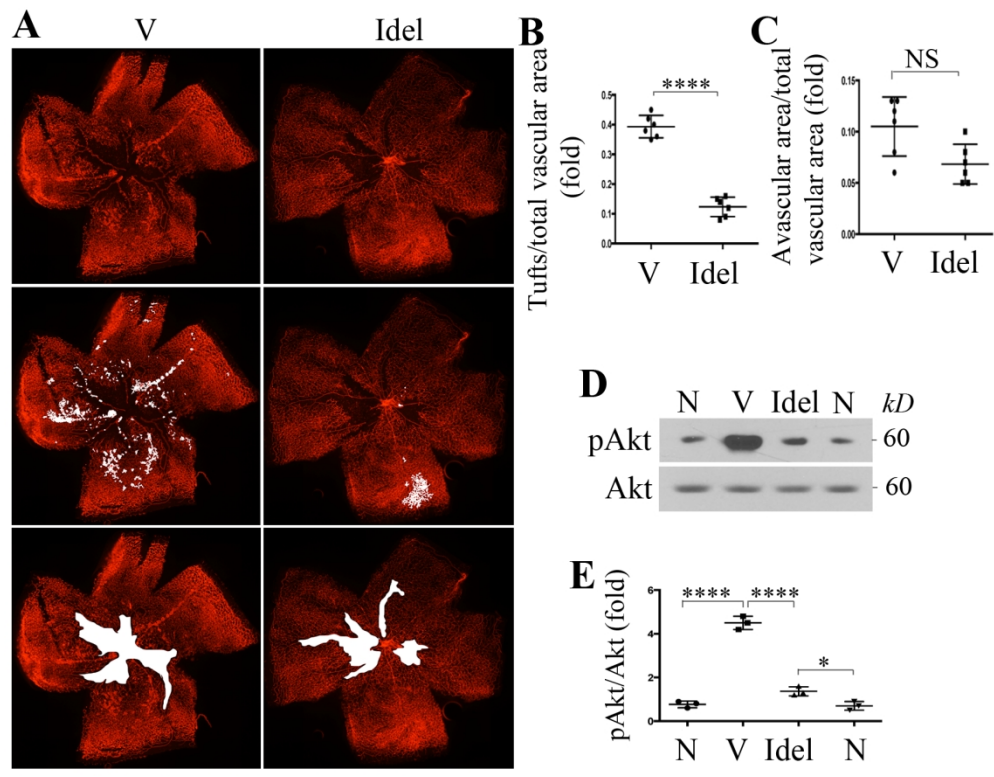








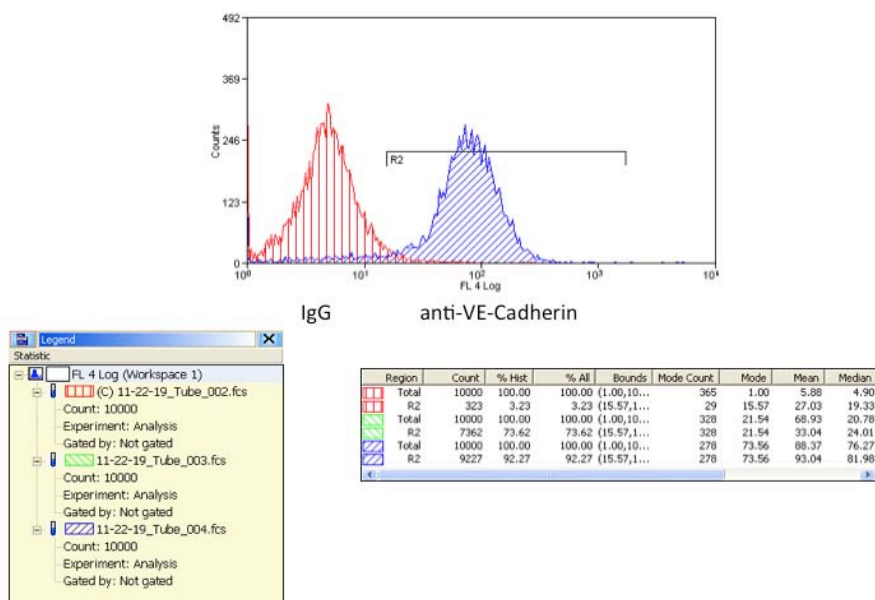




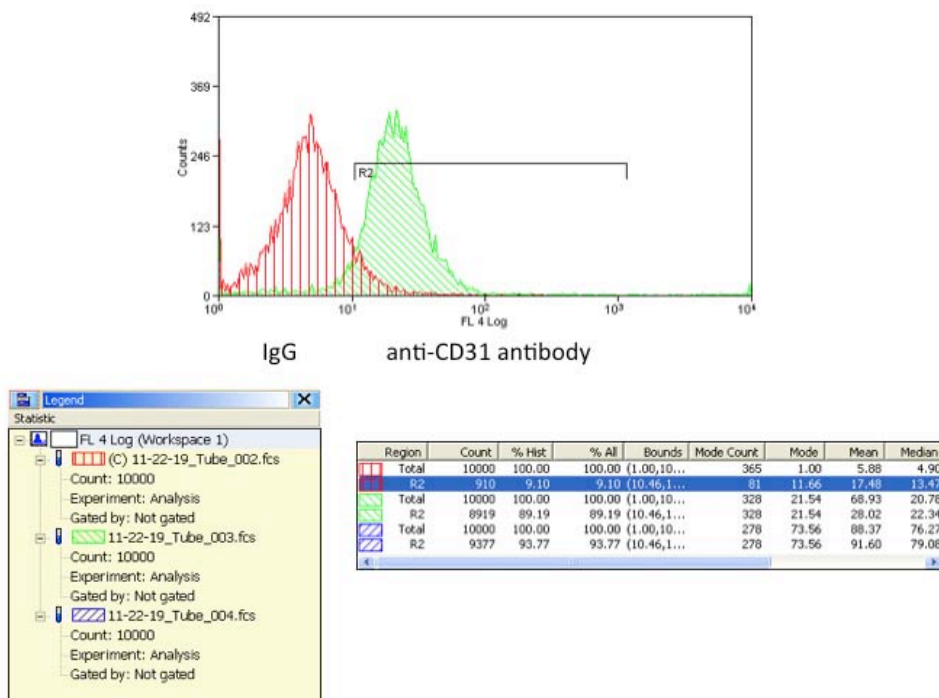
Supplementary Information

Supplementary Figure 1. Identification of human retinal microvascular endothelial cells

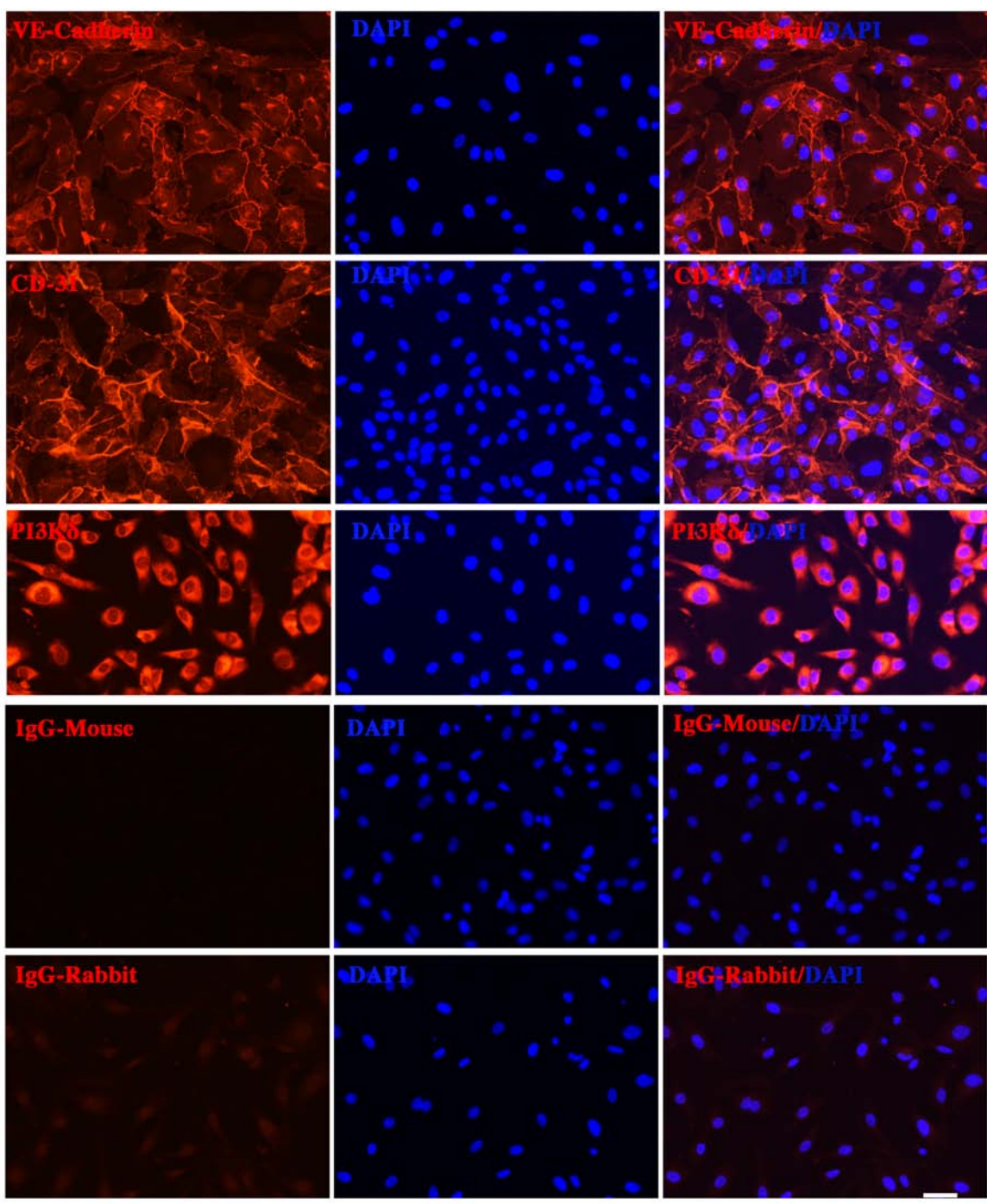
A. Flow cytometry with an antibody against VE-Cadherin



B. Flow cytometry with an antibody against CD31

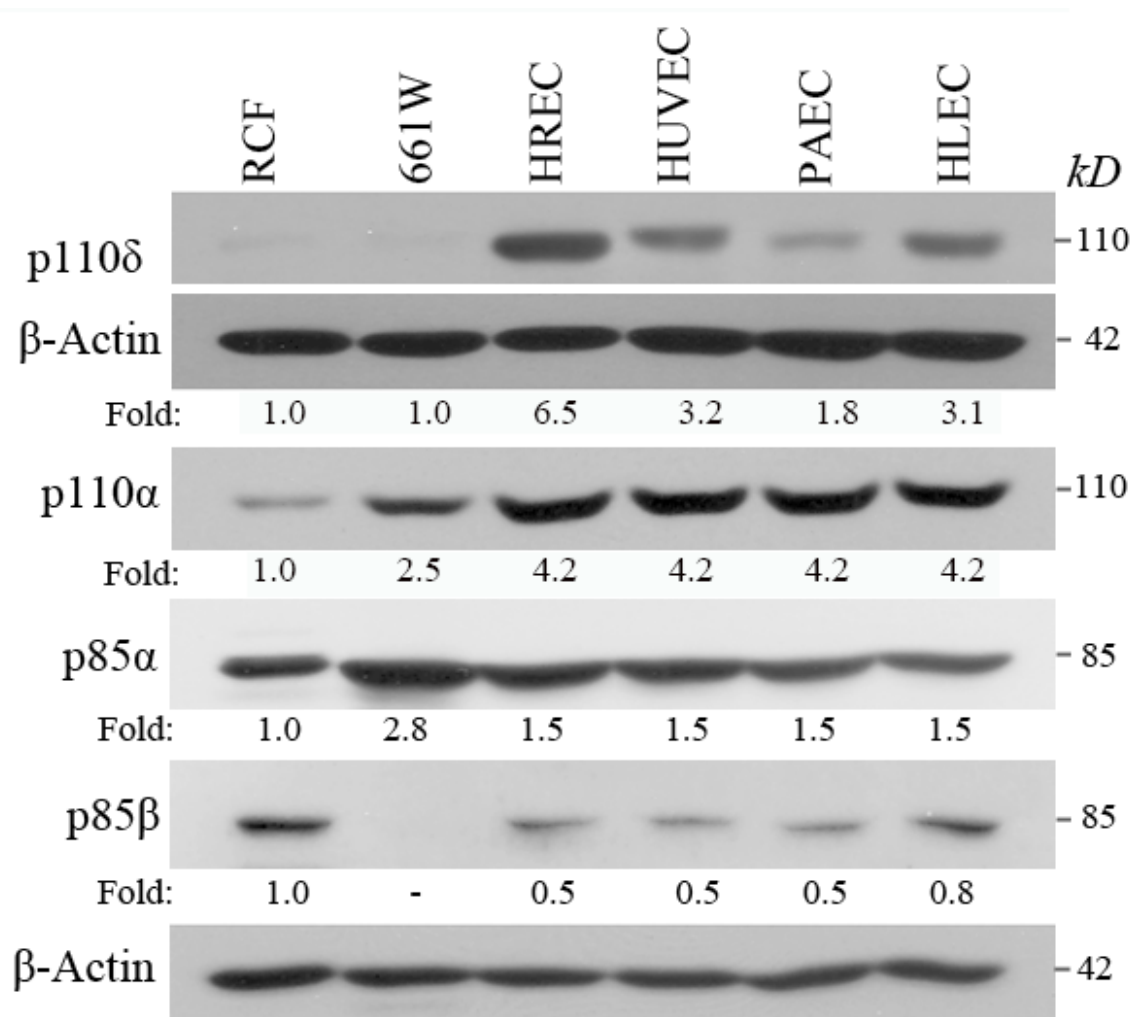


C. Immunofluorescence with antibodies against VE-Cadherin, CD31, p110 δ or non-immune IgG



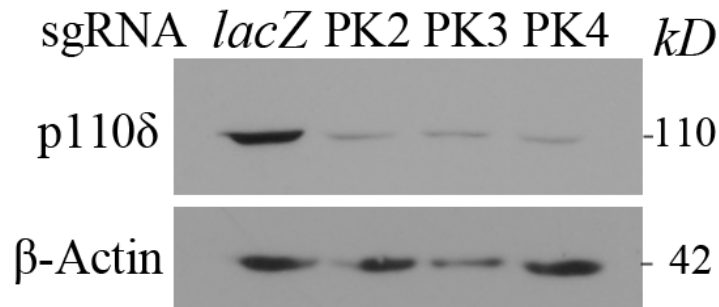
A-B. Human retinal microvascular endothelial cells (HRECs) were cultured to 80% confluence and harvested for staining with antibodies against VE-cadherin (A), CD-31 (B) or non-immune IgG (IgG) and then fluorescence-labeled secondary antibodies (Dylight 549). These stained cells were analyzed by fluorescence-activated cell sorting (FACS). This is representative of three independent experiments.

C. HRECs were cultured in a 4-well chamber to 80% confluence. After fixation with 3.7% formaldehyde, the cells were incubated with primary antibodies against VE-Cadherin, CD3, p110 δ (PI3K δ) or non-immune IgG from rabbits or mouse, and then stained with fluorescence-label secondary rabbit or mouse antibodies. This is representative of three independent experiments. Scale bar: 40 μ m.

Supplementary Figure 2. Expression of PI3K δ in vascular endothelial cells

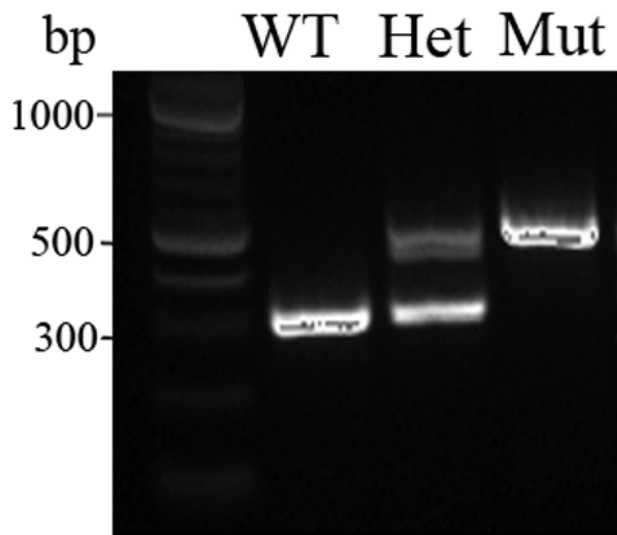
Lysates of rabbit conjunctival fibroblasts (RCFs), mouse cone photoreceptor cells (661W), human retinal microvascular endothelial cells (HRECs), human umbilical vein endothelial cells (HUVECs), porcine aortic endothelial cells (PAECs), and human lymphatic endothelial cells (HLECs) were subjected to western blot analysis using indicated antibodies. The intensity of the p110 δ and p110 α , and p85 α and - β bands was firstly normalized to that of the corresponding β -Actin bands, and then calculated to establish the ratio of the control in the first lane shown as “Fold” at the bottom of the panels. This is representative of three independent experiments.

Supplementary Figure 3. Depletion of p110 δ in HRECs using CRISPR/Cas9



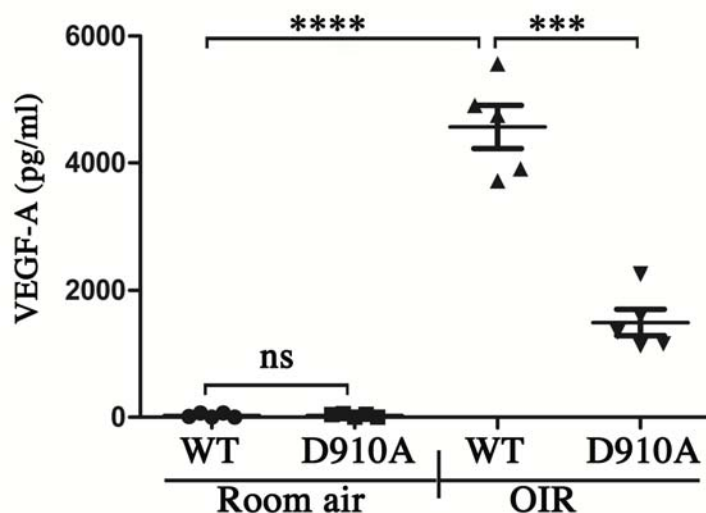
HRECs infected by lentiviruses containing SpCas9 and sgRNA-PK2, PK3 and PK4 (targeting human *PI3KCD*) or *lacZ* (targeting bacterial *lacZ*) were selected with puromycin, and their lysates were subjected to western blot using indicated antibodies. This is representative of three independent experiments.

Supplementary Figure 4. Genotyping of Mut and WT mice



Genomic DNA from tails of WT, heterozygous (Het) and Mut (mutant PI3Kp110 δ D910A/D910A) mice¹ on P12 was subjected to PCR amplification using primers (forward, P28F: CCTGCACAGAAATGCACTTCC; Reverse, P28R, AACGAAGCTCTCAGAGAAAGCTG), and separated in 1.5% agarose gel. Images were taken under ultraviolet light.

Supplementary Figure 5. Measurement of VEGF-A in the mouse vitreous



Clarified vitreous (5 μ l) from each eye of P17 mice in room air or experiencing OIR was diluted with PBS into 50 μ l, which was added into each well/a 96-well plate and subjected to a mouse VEGF 120 and 165 quantikine ELISA assay. Each group from five eyes of five mice.

WT: wild type *PIK3CD*, D910A: Mutant *PIK3CD* D910A. Room air: mice staying in room air always, OIR: mice experiencing oxygen induced retinopathy. *** and **** indicate significant difference ($p < 0.001$ and 0.0001 , respectively) using one-way ANOVA followed by the Tukey post hoc-test. ns: not significant.

Reference

1. Okkenhaug, K., *et al.* Impaired B and T cell antigen receptor signaling in p110delta PI 3-kinase mutant mice. *Science* **297**, 1031-1034 (2002).